Int. J. Multiphase Flow, Vol. 5, pp. 301–312
Pergamon/Elsevier, 1979. Printed in Great Britain

DUST ENTRAINMENT IN A SHOCK-INDUCED, TURBULENT AIR FLOW

K. BRACHT† and W. MERZKIRCH

Institut für Thermo- und Fluiddynamik, Ruhr-Universität, D-4630 Bochum, Germany

(*Received* 25 *February* 1979; *in revised form* 8 *August* 1979)

Abstract—Dust from a layer on the floor of a shock tube is entrained by the air flow behind the unsteady shock wave. The development of the dust mass concentration profiles is measured by means of an optical extinction method. The concentration profiles which can be described by an exponential law approach a stationary limit consistent with the results of pneumatic transport theory. A theoretical model simulating the dust entrainment by a diffusion process is evaluated numerically and compared with the experimental results.

1. INTRODUCTION

Dust explosions are a severe source of danger in underground coal mines. Prior to the initiation of such an explosion there occurs the formation of an air–dust mixture. The unsteady air flow behind a pressure wave or shock wave moving along the gallery of a mine may entrain the coal dust covering the floor and the walls of the gallery, thus forming the dangerous dust cloud. Since the mixture is explosive only within a certain range of values of the dust concentration in air (Palmer 1973), one is generally interested in knowing and understanding the development of the dust concentration as a function of time in the described flow.

Large-scale tests have been performed in various coal research establishments in order to obtain empirical data on some gross properties of coal dust explosions (Reeh 1971; Rae 1971; Singer *et al.* 1976). The mechanism of dust removal from a plane surface by a shock wave has been explored in a number of laboratory experiments (Fletcher 1976; Merzkirch & Bracht 1978). Hwang *et al.* (1974) proposed a theoretical model to predict the development of dust mass concentration as a function of time. This theory based on both a diffusion and a source flow model has not been investigated quantitatively, nor compared with experimental data since it makes use of a number of mass flow parameters which are not known *a priori*.

The present paper describes a series of shock tube experiments in which the dust concentration in the developing dust cloud is measured by means of an optical extinction technique. The plane dust layer originally covering the floor of the rectangular shock tube is eroded by the shock and entrained into the subsequent air flow. The shock tube and the dust used for these experiments are the same as specified in an earlier paper (Merzkirch & Bracht 1978). The dust particles have a specific weight $\rho_p = 2.9\,\mathrm{g/cm^3}$ and a mean size of diameter $D_p = 15\,\mu\mathrm{m}$. The distribution of particle sizes implies that the applied extinction technique can only yield results of limited validity. The aim of the investigations is to deduce a general representation for the development of the dust mass concentration in the unsteady shock tube flow and to compare the experimental results with the aforementioned theoretical model (Hwang *et al.* 1974).

2. OPTICAL EXTINCTION TECHNIQUE

In order to measure the dust concentration it was necessary to develop a non-disturbing experimental technique appropriate for these particular flow conditions. The total time available for the measurements is only a few milliseconds. During this period the dust mass concentration may change over several orders of magnitude. The data have to be taken with a high degree of resolution in time.

†Present address: Gesellschaft für Reaktorsicherheit, D-5000 Köln, Germany.

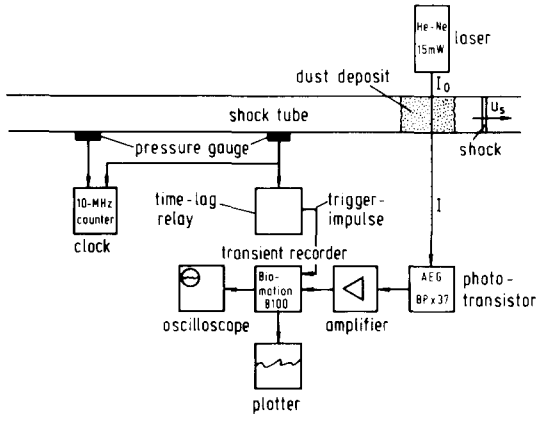

Figure 1. Optical extinction technique adopted to the shock tube.

The set-up of an extinction technique which was used for the experiments is shown in figure 1. The unexpanded beam of a He–Ne-laser is directed through the viewing windows of the optical test section of the shock tube. The beam is parallel to the plane floor of the shock tube, and it can be adjusted at various heights above the floor. A cavity in the floor of the test section, 300 mm long, is filled with dust, Before every experiment the dust surface is spread to be smooth and plane with the rest of the tube floor. When the dust cloud develops in the air flow behind a shock wave that has passed the test section, the laser light is attenuated. The light intensity is measured by a phototransistor, and the electrical signal, after magnification, is stored by a transient recorder and displayed on an oscilloscope or on a x–y recorder. The recording system is synchronized with the propagating shock wave by means of a trigger pulse generated by the shock in a piezo-electric pressure gauge. With the pulse from a second pressure gauge and a counter it is possible to determine the initial speed or strength of the shock wave.

The flow in a shock tube of rectangular cross section is, to high a degree of accuracy, plane or two-dimensional. Therefore it is assumed that the gross properties of the developing two-phase flow are also two-dimensional, i.e. they do not depend on the z-coordinate in the direction of the transmitted laser beam. The unsteady profiles of dust mass concentration $c(y, t)$ are determined at a position $x = 280$ mm down-stream of the leading edge of the dust deposit (x is the coordinate in the direction of the tube axis). For the present experimental conditions it could be shown by means of reference measurements that the concentration profiles at and beyond this distance from the leading edge are independent of x.

With the experimental arrangement shown in figure 1, one measures the relative light intensity $I^* = I/I_0$, I being the light intensity of the attenuated beam, which has the initial intensity I_0 before entering the test section. At each position y the measured light intensity is $I^* = 1$ before the edge of the dust cloud reaches this height y above the floor of the channel (Merzkirch & Bracht 1978). Then, I^* decreases continuously with time until the light is fully extinguished, i.e. $I^* = 0$ (figure 2). The measurement is finished when the shock wave reflected from the tube end-wall re-enters the test section. The profiles in figure 2 are the result of a large number of individual experiments; they are surrounded by shaded regions which represent the scatter of the experimental data. Due to this scatter the measurements will not be evaluated below $I^* = 0.1$.

In order to convert the measured light intensities of figure 2 into values of dust mass concentration a special calibration device has been developed which has been described in detail by Bracht (1978). This device is similar to the so-called Hartmann apparatus (e.g. Eggleston & Pryor 1967), in which a defined mass of dust is distributed more or less uniformly in a defined volume. Laser beam extinction measurements are performed with these known

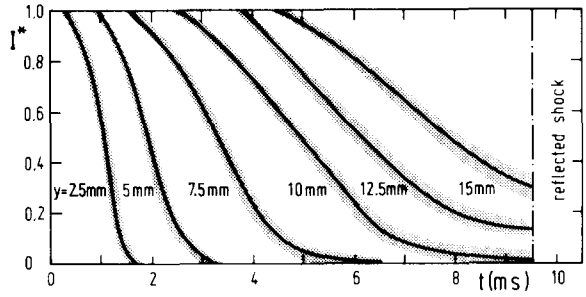

Figure 2. Measured relative light intensity $I^* = I/I_0$ as a function of time at various values of the height y above the channel floor. Distance from the leading edge of the dust deposit $x = 280$ cm; shock Mach number $M_s = 1.18$.

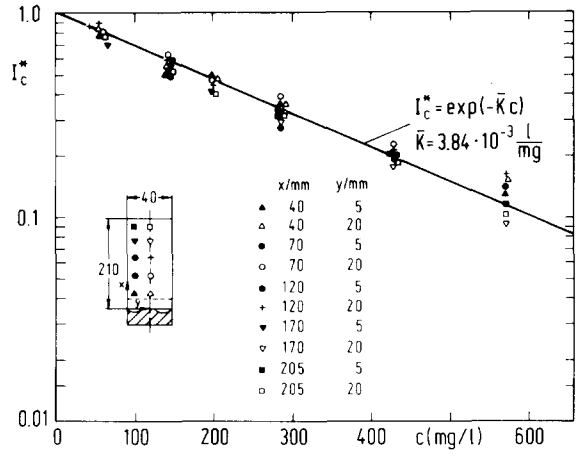

Figure 3. Calibration of the measured relative light intensity $I^* = I/I_0$ in terms of the dust mass concentration c. Symbols indicate the various position x, y on the calibration device through which the laser beam has been directed. Dust as specified by Bracht (1978).

values of dust mass concentration c, resulting in the calibration curve of figure 3. The exponential behaviour

$$I^* = \exp(-\bar{K} \cdot c) \qquad [1]$$

with $\bar{K} = \text{const}$ verifies Lambert–Beer's law of light extinction, although a distribution of particle sizes is present. However, since the measurements are taken within very short periods of time, differences in the sink velocities of the various particles will not yet become effective. (Merzkirch & Bracht 1978). The mean value $\bar{K}$ only applies to this particular size distribution. The various symbols in figure 3 indicate that the laser beam is transmitted at various positions through the calibration apparatus.

3. DUST MASS CONCENTRATION PROFILES

With the aid of the calibration procedure it is possible to convert the light extinction measurements into values of dust mass concentration. Figure 4 is the result for the flow condition specified by the shock Mach number $M_s = 1.18$. Designating the dust concentration with $\bar{c}$ indicates that one measures a mean value, averaged over the high frequency turbulent fluctuations and averaged also due to the assumption of a two-dimensional flow. The time scale is based on $t = 0$ for the arrival of the shock wave at the position x of the measurement. The increase of $\bar{c}$ with time is slower, the higher the position of measurement above the channel floor. These measurements have been performed for three different shock strengths, namely $M_s = 1.29$, $M = 1.18$ and $M_s = 1.10$. The respective velocities of the undisturbed air flow behind these shocks are

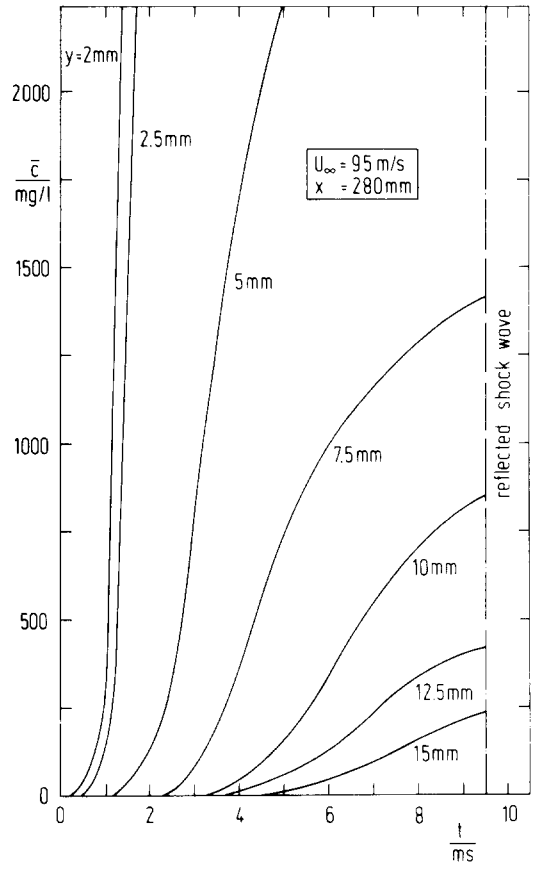

Figure 4. Mean dust concentration $\bar{c}$ as function of time for various values of the height y above the channel floor. Shock Mach number $M_s = 1.18$.

$U_\infty = 149$ m/s, $U_\infty = 95$ m/s, and $U_\infty = 58$ m/s. The scatter of the shock strenghts in the individual experiments, i.e. the degree of repeatability, is about 1%.

Cross-plotting the data of figure 4 by exchanging the parameter (height y above the channel floor) with the abscissa (time) allows one to recognize a functional behavior of the experimental results. From the semi-logarithmic representation of figure 5, again for $M_s = 1.18$, one deduces the following exponential law which describes the mean dust concentration $\bar{c}$ at a height y above the dust deposit as a function of time t:

$$\bar{c}(y, t) = \bar{c}_0(t) \cdot \exp[-\alpha(t) \cdot y]. \qquad [2]$$

The same exponential law follows from an evaluation of the experiments performed under the two other flow conditions. The shape of the functions $\bar{c}_0(t)$ and $\alpha(t)$ which both depend on the initial flow conditions (shock strength) can be obtained from an extrapolation of figure 5.

$\alpha(t)$ is found from the slopes of the straight lines in figure 5. By introducing the reduced time coordinate $\gamma = U_\infty \cdot t$ it is possible to correlate the results for the three different flow conditions so that they fit into one curve (figure 6). It should be emphasized that the numerical values for α as well as for $\bar{c}_0$ must depend on the properties of the dust; this dependence is not investigated further in this paper. From figure 6 one might conclude that α approaches a finite limit $\alpha(\infty) > 0$ for $t \to \infty$. This limit value for α cannot be zero, since $\alpha = 0$ stands for uniform dust concentration across the whole cross section of the channel. The latter is not possible due to the existence of a dust layer on the channel floor.

The dust concentration close to the floor is so high that the extinction measurements here fail to deliver reliable results. Therefore $\bar{c}_0(t)$ can be determined by extending the straight lines

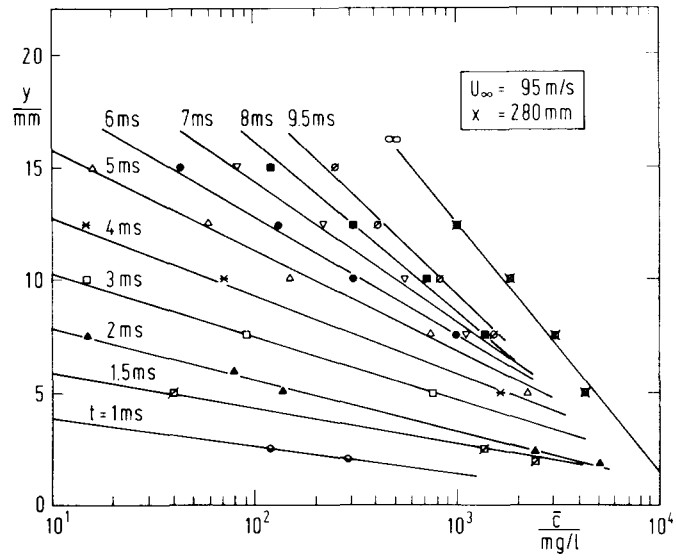

Figure 5. Mean dust concentration $\bar{c}$ as function of the height y above the channel floor as obtained by cross-plotting the data of figure 4. The parameter t is the time after the passage of the shock wave at the leading edge of the dust deposit. Shock Mach number $M_s = 1.18$.

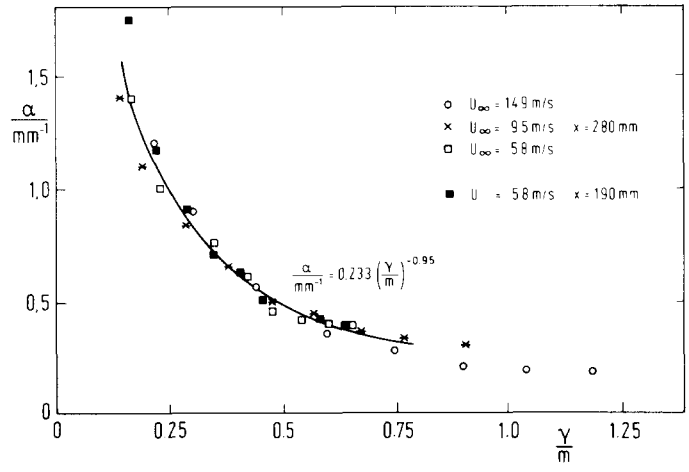

Figure 6. α according to [2] as a function of the non-dimensional time coordinate $\gamma = U_\infty \cdot t$. Symbols indicate three different shock strengths.

in figure 5 until they intersect with the abscissa ($y = 0$). The values of $\bar{c}_0(t)$ extrapolated in this way can be fitted by a curve for each shock strength (figure 7). Here it becomes necessary to ask for the physical significance of $\bar{c}_0(t)$. The values of $\bar{c}_0(t)$ are interpreted to be the dust mass concentration in an infinitesimal height ($y \to 0$ but $y > 0$) above the floor. From this assumption it follows that the fitting curve in figure 7 must originate from the point $\bar{c}_0 = 0$, $t = 0$: no dust is raised at $t = 0$. The values given for $\bar{c}_0$ are about one order of magnitude smaller than the specific weight of the dust used.

For the three flow conditions, $\bar{c}_0(t)$ passes through an early maximum, then decreases and apparently approaches a limiting value for $t \to \infty$. This behavior can be explained with the different mechanisms being responsible for the dust erosion in the laminar and in the turbulent stage of the shock tube flow. The interaction of the dust deposit with the initially thin, laminar shock tube boundary layer (Merzkirch & Bracht 1978) causes a strong lift force acting on the particles in the dust layer so that they raise by a small amount, but they cannot be entrained at the same rate by the (still) laminar air flow. With increasing degree of turbulence the dust can

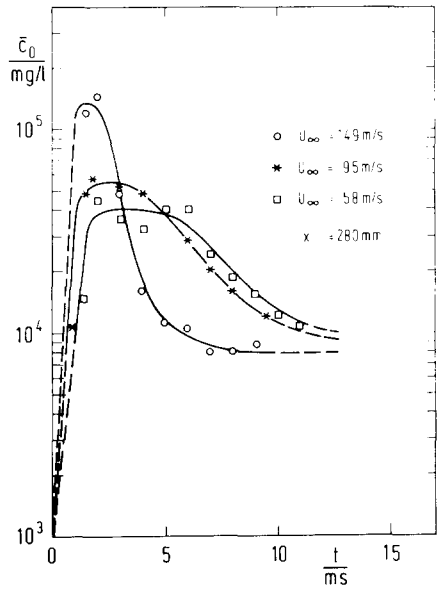

Figure 7. Extrapolated values $\bar{c}_0$ according to [2] as function of time for three different shock strengths.

be distributed at a higher rate in the air flow. At the same time the intense erosion of dust as caused in the laminar phase decreases, i.e. $\bar{c}_0$ decreases after having passed the maximum. Finally a stage of equilibrium is reached when all the dust raised due to an interaction with the turbulent boundary layer can be entrained by the turbulent channel flow. The photographs taken by Bracht (1978) confirm that this channel flow soon becomes turbulent. Figure 7, thus, is a further confirmation of the mechanism of dust erosion in the initial, laminar stage, as described in an earlier paper (Merzkirch & Bracht 1978).

It is apparent that both $\bar{c}_0(t)$ and $\alpha(t)$ asymptotically approach constant values for $t \to \infty$, so that, according to [2], also $\bar{c}(y, t)$ will have a stationary limit for $t \to \infty$. The time available for the measurements, however, is not long enough to yield reliable results for this stationary dust profile $\bar{c}(y, \infty)$. Therefore, an attempt has been made to estimate the order of magnitude of this limit: Subsequent to their apparent change in curvature, the curves in figure 4 are extended by exponential profiles. For larger values of t there is only very little change in $\bar{c}$ according to these profiles, and the value of $\bar{c}$ extrapolated in this way for $t = 100$ ms is considered as the stationary limit and inserted into figure 5 with the parameter ∞.

It is possible to compare these extrapolated stationary dust profiles with the results of the stationary pneumatic transport theory. Such an analysis has been developed by Kriegel (1967) who determines, on the basis of Prandtl's mixing-length hypothesis, the distribution of the solid phase in the turbulent fluid flow within a pipe. According to Kriegel the mean concentration $\bar{c}$ of the solid phase as a function of a non-dimensional height y^* above the floor of the channel is given by

$$\bar{c}/\bar{c}_0 = \exp(K \cdot y^*), \qquad [3]$$

$\bar{c}_0$ being the mean local concentration of the solid phase on the floor, K a constant which must be derived empirically. y^* depends on a number of numerical parameters, e.g. Reynolds number, drag coefficient of the particles (spheres), particle diameter (see [37] in Kriegel's paper), which all can be supplied for the present problem. K must be determined from the stationary limit included in figure 5. The details of this matching process and of supplying the necessary parameters for y^* are reported by Bracht (1978). Since K is determined for the shock Mach number $M_s = 1.18$, the results according to [2] and [3] coincide for this particular flow condition. Applying the same K to the two other shock strengths results in only little

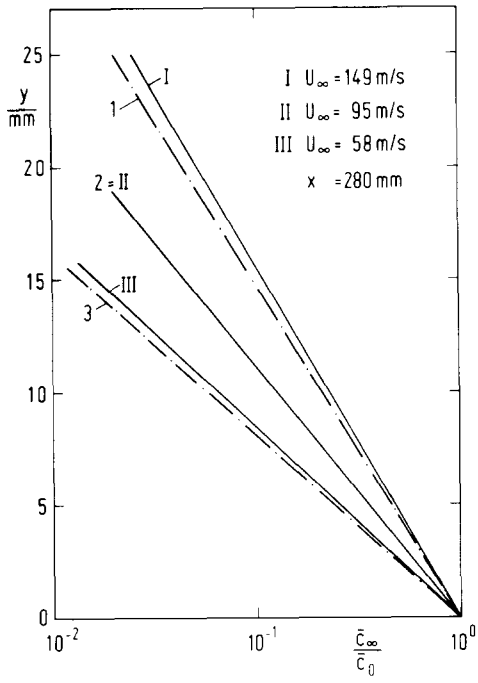

Figure 8. Stationary limit ($t \to \infty$) of dust mass concentration, $\bar{c}_\infty$, as a function of the height y above the channel floor. Comparison of the results extrapolated from the measurements (I, II, III) with the pneumatic transport theory (1, 2, 3) ([3]).

divergence between the stationary limit of the present experiments and the predictions according to the stationary pneumatic transport theory (figure 8). This may be considered as an evidence that the stationary limits ($t \to \infty$) in figures 5–7 do exist and are determined to within the correct order of magnitude.

4. COMPARISON WITH THE RESULTS OF THE THEORETICAL DIFFUSION MODEL

Hwang *et al.* (1974) present a theoretical model for predicting the dust concentration as a function of time. The entrainment of the eroded dust by the air flow in the shock tube is considered to be a turbulent diffusion process. The dust layer on the floor acts as a source releasing a stream of dust which mixes with the air stream. The intensity of this source as well as the diffusion coefficients are not known *a priori*, and need to be determined by fitting the theoretical solution with the experimental results. Such evaluation of the theoretical model by Hwang *et al.* will be described only in brief. Again, the details of this complicated numerical procedure are reported by Bracht (1978).

Considering the dust mass concentration c to be composed of a mean value $\bar{c}$ and a fluctuating component c',

$$c(x, y, t) = \bar{c} + c',$$

one derives for the diffusion of the solid phase in a two-dimensional, turbulent fluid flow the following equation (e.g. Roohsenow and Chou 1963):

$$\frac{\partial \bar{c}}{\partial t} + \bar{u}\frac{\partial \bar{c}}{\partial x} + \bar{v}\frac{\partial \bar{c}}{\partial y} = \frac{\partial}{\partial x}\left(D\frac{\partial \bar{c}}{\partial x} - \overline{u'c'}\right) + \frac{\partial}{\partial y}\left(D\frac{\partial \bar{c}}{\partial y} - \overline{v'c'}\right) \qquad [4]$$

$\bar{u}$, $\bar{v}$ are the mean flow velocities in the x- and y-direction, respectively; u', v' the turbulent velocity fluctuations; D the molecular diffusion coefficient. The solution of the problem may be

facilitated by means of the following assumptions: The expressions for the turbulent flux, $\overline{u'c'}$, $\overline{v'c'}$, are replaced by

$$\overline{u'c'} = -k_x \frac{\partial \bar{c}}{\partial x}, \overline{v'c'} = -k_y \frac{\partial \bar{c}}{\partial y}. \qquad [5]$$

For a first approach the values of the eddy mass diffusivity, k_x and k_y, are taken as constant; this is surely not the case near a wall (see below). After the passage of the shock wave, the mean flow velocity is uniform: $\bar{u} = U_\infty = \text{const}$, $v = 0$. Neglecting the molecular diffusion ($D = 0$) results in

$$\frac{\partial \bar{c}}{\partial t} + \bar{u} \frac{\partial \bar{c}}{\partial x} = k_x \frac{\partial^2 \bar{c}}{\partial x^2} + k_y \frac{\partial^2 \bar{c}}{\partial y^2}. \qquad [6]$$

Solving [6] requires prescription of a set of initial and boundary conditions. The initial condition (index A) is given in form of a system of sources which simulate the dust layer of length 1 and width b on the channel floor:

$$\bar{c}_A(x, y, t_1) = 0 \quad \text{for} \quad \begin{cases} x < 0, y \\ x > 1, y \\ 0 \leq x \leq 1, y > 0 \end{cases}$$

$$\bar{c}_A(x, y, t_1) = \infty \quad \text{for} \quad 0 \leq x \leq 1, y = 0$$

In each point of the interval $0 \leq x \leq 1$ the dust source is initiated by the shock wave that propagates with the velocity u_s and passes the leading edge of the dust layer ($x = 0$) at time $t = 0$. This initiation of the source activity is expressed by the second condition (above); the instantaneous peak of the dust mass concentration at time t_1 can be described in terms of a Dirac function. The peak of dust concentration propagating across the interval $0 \leq x \leq 1$ represents a mass source of intensity $\phi\ (x, t_1)$ being active continuously during the time period $0 \leq t_1 \leq t$. The source intensity ϕ is defined by the following assumption: The dust concentration $c\ (x, y, t)$ integrated over the total volume of the channel from $x = -\infty$ to $x = \infty$ yields a finite value; this is the amount of dust mass m released by the source up to this instant of time t:

$$b \int_{-\infty}^{+\infty} \int_0^a c(x, y, t)\, \mathrm{d}y\, \mathrm{d}x = \int_0^1 \int_0^t \phi(x, t_1)\, \mathrm{d}t_1\, \mathrm{d}x = m(t) \qquad [7]$$

b is the width (in z-direction) and a the height (in y-direction) of the shock tube channel.

For greater simplicity ϕ might be assumed to be constant. Then, [4] has an analytic solution valid for constant values of k_x, k_y, and ϕ (e.g. Carslaw & Jaeger 1967):

$$\bar{c}(x, y, t) = \frac{\phi}{2ab}\left[\int_0^{t_1} \left\{1 + 2\sum_{m=1}^{\infty} \exp\left[-k_y m^2 \pi^2 (t - t_1)/a^2\right] \cos\frac{m\pi y}{a}\right\} \{\mathrm{erf}\,[\psi(0)] - \mathrm{erf}\,[\psi(u_s t_1)]\}\, \mathrm{d}t_1 \right.$$

$$\left. + \int_{t_1}^{t} \left\{1 + 2\sum_{m=1}^{\infty} \exp\left[-k_y m^2 \pi^2 (t - t_1)/a^2\right] \cos\frac{m\pi y}{a}\right\} \{\mathrm{erf}\,[\psi(0)] - \mathrm{erf}\,[\psi(1)]\}\, \mathrm{d}t_1\right] \qquad [8]$$

with

$$\psi(x_1) = \frac{x - x_1 - \bar{u}(t - t_1)}{2\sqrt{(k_x(t - t_1))}} \text{ and } t_1 = 1/u_s.$$

The evaluation of [8] requires knowledge of numerical values of k_x, k_y and ϕ; however, such values are not available. The influence of these parameters on the solution [8] has been

investigated in a series of numerical tests. The results in brief: k_x has no significant influence because the mass diffusion in axial direction (x) is very small as compared with diffusion in the vertical direction (y). Therefore, k_x has been taken constant in all cases and about one order of magnitude smaller than typical values of k_y (see below). The mass concentration profiles according to [8] vary only very little with time. This is in contrast to the experimental findings, as represented in figure 5, where the time is indicated by the parameter of the curves.

Plotting the $\bar{c}$-profiles in the same semi-logarithmic scale as in figure 5 results in a further difference in the experimental and the numerical results: the calculated profiles are curved and not straight as in figure 5. However, if one excludes a small regime close to the floor where $\bar{c}$ reaches high values, the calculated profiles can be approximated by straight lines to within a certain degree of accuracy. This is indicated in figure 9 for the shock strength $M_s = 1.18$. The calculations are made independent of the value of ϕ by using the relative dust concentration $\bar{c}/\bar{c}_0$. The calculated profiles are evaluated for the time coordinate $t = 5$ ms and with different values of k_y. Comparing figures 5 and 9 suggests that the assumption of constant values of k_y cannot provide agreement between the diffusion model and the experiments; k_y should rather be a function of time. In addition, k_y also will strongly depend on y near the wall as one might conclude from the pattern of the curves in figure 9 for small values of y.

It is possible to determine the function $k_y = f(t)$ by comparing directly the parameters in figures 5 and 9, although the profiles in figure 9 have been calculated under the assumption of constant values of k_y. This is a consequence of the particular dependence of the solution [8] on the time coordinate which can be expressed by saying that $\bar{c}$ has "poor memory". The difference of the two error functions in [8] causes that the value of $\bar{c}$ for an instant of time t_1 is determined by the constant value of k_y only within a small interval $|t_1 - t|$, while any variation of k_y outside of this interval does not affect the solution (Bracht 1978). One may thus apply the solution [8] to the present problem that is characterized by time-dependent values of the eddy mass diffusivity k_y, and it becomes necessary to derive $k_y(t)$ from the described comparison of the experimental and calculated $\bar{c}$-profiles. The values of k_y for the three shock strengths used in the experiments can be correlated by defining reduced expressions $K = k_y/(\bar{u} \cdot a)$ and $T = (\bar{u} \cdot t)/a$ (figure 10). Only for large values of the reduced time coordinate T, K depends on the shock strength (expressed by M_s or $\bar{u}$).

No empirical information is available on how the source intensity ϕ varies with time, and determining $\phi(t)$ requires a similar procedure as that used for deriving $k_y(t)$. From physical arguments it follows that ϕ, too, must be a function of time, and $\phi(t)$ is found by comparing figure 5 with a diagram in which the absolute concentration according to [8] has been plotted for

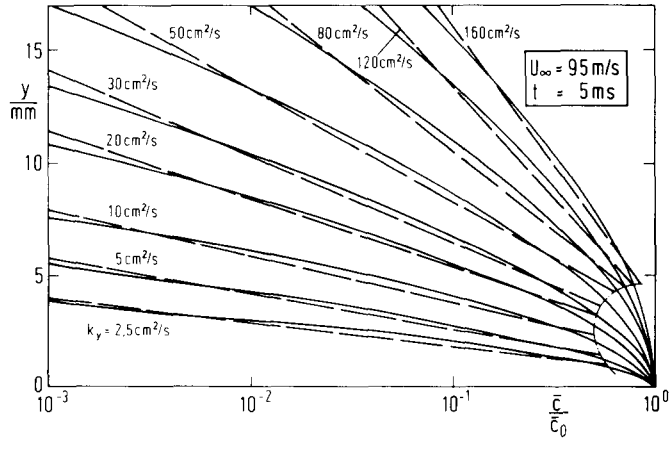

Figure 9. Relative concentration profiles evaluated from [8] for different values of the eddy mass diffusivity k_y. The theoretical curves (——) can be approximated by straight lines (– – –) except for a small regime close to the wall. Shock Mach number $M_s = 1.18$.

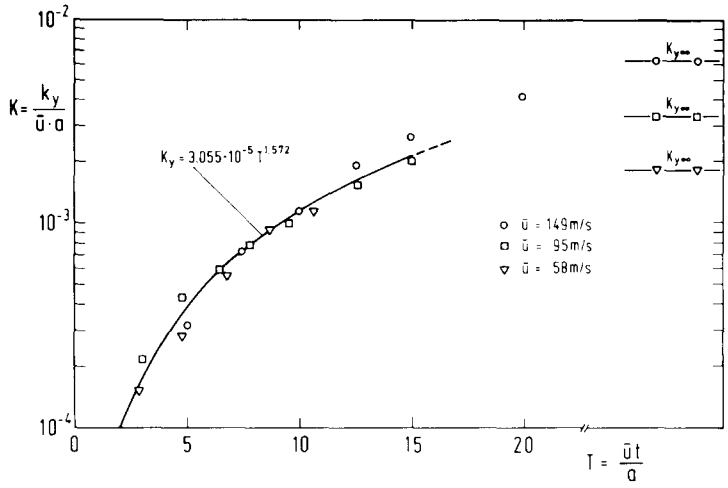

Figure 10. Non-dimensional eddy mass diffusivity K as function of the non-dimensional time coordinate T for three different shock strengths.

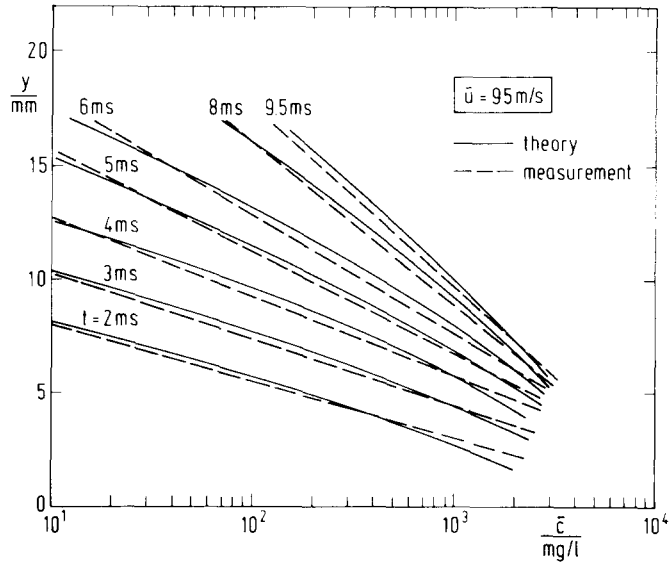

Figure 11. Comparison of the absolute dust concentration profiles according to [8] (——) with the measured profiles (– – –). Shock Mach number $M_s = 1.18$.

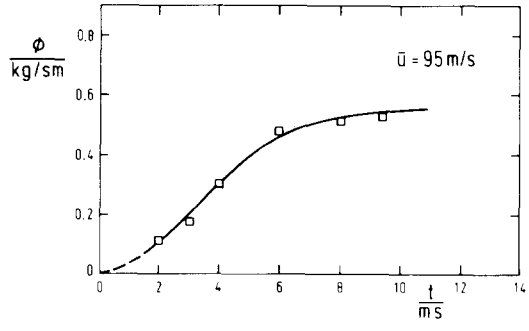

Figure 12. Dust source intensity ϕ as function of time as obtained after matching the diffusion theory [8] to the measured absolute concentration profiles.

variable $k_y(t)$ (figure 11). The resulting pattern for $\phi(t)$ (figure 12) provides a criterion for checking whether the described procedure with the many degrees of arbitrariness and the numerical results are reasonable. As one might expect, $\phi(t)$ approaches a nearly constant value some time after the initiation of the source. Integration of the curve $\phi(t)$ delivers the amount of dust mass which has been released from the deposit up to a certain instant of time. For the experimental condition referred to in figure 12, a mass of 1 g dust has been eroded after 10 ms, while the total mass of dust filled into the deposit was 7 g. These two numerical values appear to be in good agreement.

5. DISCUSSION

The experiments have been performed to search for a possibility for predicting the development of dust mass concentration in the described unsteady air flow. The results show that the prediction can be made either with the aid of the diffusion theory proposed by Hwang *et al.* (1974) or with the empirical equation [2] which can be put in a non-dimensional form to fit all experimental conditions that have been varied here. However, both possible ways depend on a number of data which can be determined only by means of experiments. These data, particularly, are the time-dependent eddy mass diffusivity $k_y(t)$ and the mass source intensity $\phi(t)$ for the diffusion model, and the functions $\alpha(t)$ and $c_0(t)$ in [2]. From the preceding definitions and arguments, and since α is proportional to the gradient $\partial c/\partial y$, it follows that there is a physical correspondence between k_y and α, and between ϕ and c_0, respectively.

The only means, so far, to provide the referred data is to perform the shock tube experiments described in this paper. In this way, the pattern of $\alpha(t)$ and $c_0(t)$ is determined directly, and it appears not necessary to use these data for matching the values of $k_y(t)$ and $\phi(t)$ and to evaluate the rather complicated diffusion theory, since [2] already provides a reasonable representation of the desired concentration profiles. Furthermore, for large value of time, i.e. $t \to \infty$, the measured pattern of $\alpha(t)$ and $c_0(t)$ indicates that [2] is in good agreement with other existing results, whereas the diffusion theory would predict a uniform distribution of the dust over a cross-section of the channel. However, the fact that the measurements are compatible with the diffusion model can be seen as a proof that the experimental results are of a general physical nature.

The values derived for α, c_0 as well as those for k_y, ϕ are specific values associated with the dust used in these experiments. As stated earlier, coal dust is inconvenient to be used in a shock tube. Repeating the measurements with different sorts of dust could enable one to extrapolate the desired information for coal dust. Number values of the eddy mass diffusivity, as needed in the above diffusion theory, have been measured for a few particle/fluid combinations only and under stationary flow conditions. Further shock tube experiments with different sorts of dust would therefore contribute not only to the safety problem in coal mines as mentioned in the introduction but also to the general understanding of the entrainment mechanism in a turbulent flow.

Acknowledgement—This research has been supported by a grant from Minister für Wissenschaft und Forschung des Landes Nordrhein-Westfalen.

REFERENCES

BRACHT, K. 1978 Eine Untersuchung zur zeitlichen und örtlichen Entwicklung eines Staub-Luft Gemisches in einer stoßinduzierten Strömung. Dissertation, Ruhr-Universität Bochum.

CARSLAW, H. S. & JAEGER, J. C. 1967 *Conduction of Heat in Solids.* Oxford University Press.

EGGLESTON, L. A. & PRYOR, A. J. 1967 The limits of dust explosibility. *Fire Techn.* **3**, 77–89.

FLETCHER, B. 1976 The interaction of a shock with a dust deposit. *J. Phys. D: Appl. Phys.* **9**, 197–202.

HWANG, C. C., SINGER, J. M. & HARTZ, T. N. 1974 Dispersion of dust in a channel by a turbulent gas stream. U.S. Bureau of Mines, Pittsburgh, PA, Rep. Invest. 7854.

KRIEGEL, E. 1967 Konzentrationsprofile beim hydraulischen Transport feinkörniger Feststoffe. VDI-Fortschr. Ber. Reihe 13, Nr. 9, VDI-Verlag Düsseldorf.

MERZKIRCH, W. & BRACHT, K. 1978 The erosion of dust by a shock wave in air: Initial stages with laminar flow. *Int. J. Multiphase Flow* **4**, 89–95.

PALMER, K. N. 1973 *Dust Explosions and Fires.* Chapman & Hall, London.

RAE, D. 1971 Coal-dust explosions in large tubes. Shock Tube Research. In *Proc. 8th Int. Shock-Tube Symp.*, pp. 47/1–11. Chapman & Hall, London.

REEH, D. 1971 Versuche über den Ablauf von Kohlestaubexplosionen in Druckgefässen und in einer 200 m langen Rohrstrecke NW 1800. Staub-Reinhalt. *Luft* **31**, 101–107.

ROHSENOW, W. M. & CHOU, H. 1963 *Heat, Mass and Momentum Transfer.* Prentice Hall, London.

SINGER, J. M., HARRIS, M. E. & GRUMER, J. 1976 Dust dispersal by explosion-induced airflow. U.S. Bureau of Mines, Pittsburgh, PA, Rep. Invest. 8130.